BIOCHEMISTRY
including biophysical chemistry & molecular biology

ARTICLE

pubs.acs.org/biochemistry

Internal Dynamics of the Tryptophan Repressor (TrpR) and Two Functionally Distinct TrpR Variants, L75F-TrpR and A77V-TrpR, in Their L-Trp-Bound Forms

Brian P. Tripet, Anupam Goel, and Valérie Copié*

Department of Chemistry and Biochemistry, Montana State University, Bozeman, Montana 59717, United States

Supporting Information

ABSTRACT: Backbone amide dynamics of the *Escherichia coli* tryptophan repressor protein (WT-TrpR) and two functionally distinct variants, L75F-TrpR and A77V-TrpR, in their holo (L-tryptophan corepressor-bound) form have been characterized using ^{15}N nuclear magnetic resonance (NMR) relaxation. The three proteins possess very similar structures, ruling out major conformational differences as the source of their functional differences, and suggest that changes in protein flexibility are at the origin of their distinct functional properties. Comparison of site specific ^{15}N-T_1, ^{15}N-T_2, ^{15}N-{^{1}H} nuclear Overhauser effect, reduced spectral density, and generalized order (S^2) parameters indicates that backbone dynamics in the three holo-repressors are overall very similar with a few notable and significant exceptions for backbone atoms residing within the proteins' DNA-binding domain. We find that flexibility is highly restricted for amides in core α-helices (i.e., helices A−C and F), and a comparable "stiffening" is observed for residues in the DNA recognition helix (helix E) of the helix D−turn−helix E (HTH) DNA-binding domain of the three holo-repressors. Unexpectedly, amides located in helix D and in adjacent turn regions remain flexible. These data support the concept that residual flexibility in TrpR is essential for repressor function, DNA binding, and molecular recognition of target operators. Comparison of the ^{15}N NMR relaxation parameters of the holo-TrpRs with those of the apo-TrpRs indicates that the single-point amino acid substitutions, L75F and A77V, perturb the flexibility of backbone amides of TrpR in very different ways and are most pronounced in the apo forms of the three repressors. Finally, we present these findings in the context of other DNA-binding proteins and the role of protein flexibility in molecular recognition.

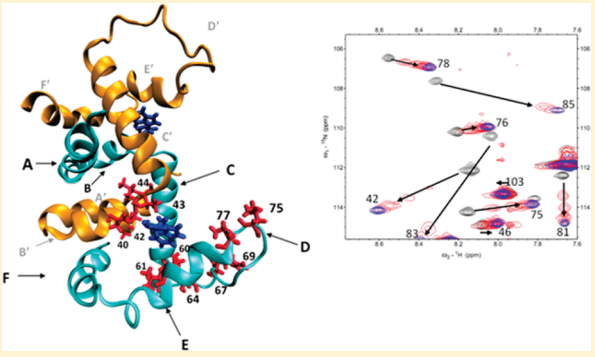

The tryptophan repressor protein (TrpR) of *Escherichia coli*, a DNA-binding protein, regulates the transcription of genes whose protein products are involved in the biosynthesis of aromatic amino acids such as L-tryptophan (L-Trp) and others. The activity of TrpR is regulated by the intracellular concentration of its corepressor L-Trp. When cellular levels of L-Trp are low, the unliganded form of the repressor (apo-WT-TrpR) displays low affinity for specific operator DNA targets. As the intracellular concentration of L-Trp increases, dimeric TrpR binds two molecules of L-Trp, resulting in an activated L-Trp-bound holo-repressor. The activated holo-WT-TrpR binds with high affinity to operator targets upstream of the *aroH*, *aroL trpEDCBA*, *mtr*, and *trpR* operons and represses the transcription of these operon-encoded genes.[1−4]

The structure of TrpR has been examined extensively by X-ray[5−7] and solution nuclear magnetic resonance (NMR) techniques.[8,9] TrpR is a 25 kDa homodimer with each subunit comprising two identical 108-residue polypeptide chains.[10] Structural data have indicated that each subunit consists of six α-helices labeled A−F (Figure 1A). Helices A−C and F of the two subunits associate to form an intertwined dimer and the hydrophobic core of the protein, while α-helices D and E comprise the helix−turn−helix (HTH) DNA-binding domain of each TrpR subunit. Structural investigations have shown that the core α-helices of TrpR are well-ordered while the DNA-binding domains (two per dimeric TrpR) protrude as less-ordered flexible extensions from a more motionally restrained protein core.[11,12] Analysis of the solution structures of apo- and holo-WT-TrpR suggested that binding of L-Trp to the apo-repressor results in a sequential ordering of the protein's helix D−turn−helix E (HTH) DNA-binding domains, as evidenced by the observation of additional intrahelical NMR ^{1}H-^{1}H nuclear Overhauser effects (nOes) particularly within the helix E region of holo-WT-TrpR that were absent in apo-WT-TrpR,[9] of slower backbone amide proton ^{1}H/^{2}H exchange rates, and of changes in ^{1}H NMR relaxation time constants.[13−15] Small but significant structural changes upon formation of holo-WT-TrpR result in the repositioning of the helices E further apart so as to fit into two

Received: March 16, 2011
Revised: May 5, 2011
Published: May 09, 2011

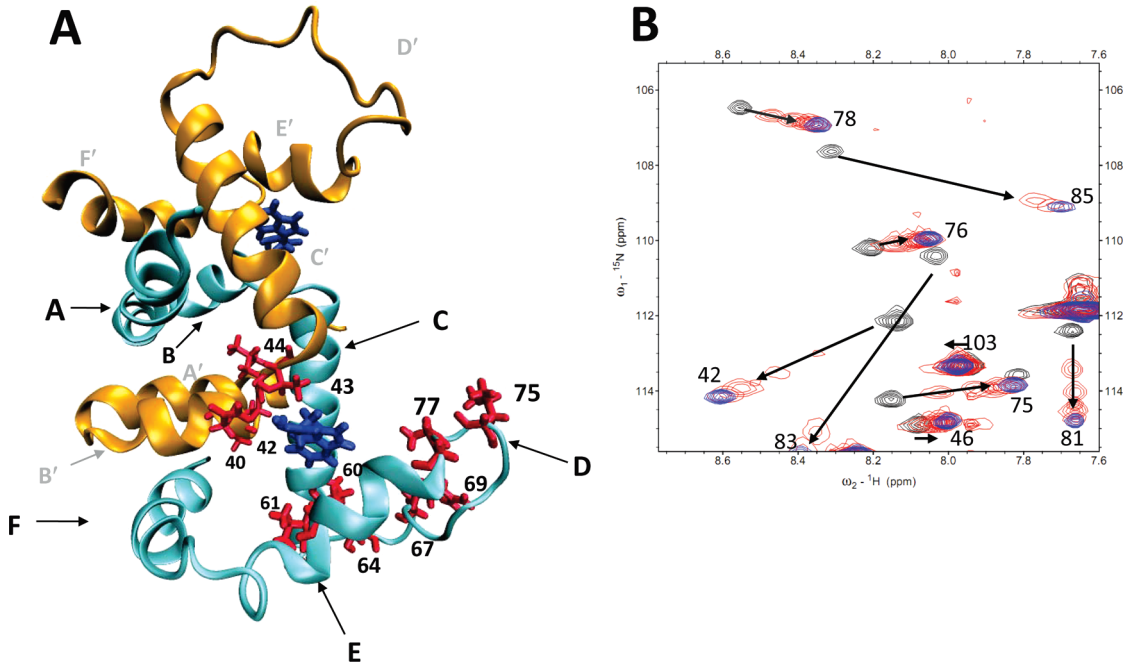

Figure 1. (A) Ribbon representation of the structural elements of holo-WT-TrpR. The backbone structures of the two subunits are colored gold and light blue, with helices A−E labeled. The L-tryptophan corepressor is colored blue in stick representation. Side chains corresponding to amides with the most perturbed $^{15}N/^{1}H$ chemical shifts upon L-Trp binding (i.e., residues 40, 42, 43, 60, 61, 64, 67−69, 75, 77, and 85) are colored red and shown in stick representation. The TrpR protein model was built using the molecular graphics program VMD, version 1.8.3, and the solution NMR structure of WT-TrpR (PDB entry 1WRS). (B) Section of an overlay of two-dimensional $^{1}H/^{15}N$ HSQC spectra displaying the change in the $^{1}H/^{15}N$ chemical shift of several residues upon titration of L-Trp into WT-TrpR. Resonance assignments are shown along with arrows indicating the directions of chemical shift changes. Contour levels colored gray correspond to the location of $^{1}H/^{15}N$ resonances of apo-WT-TrpR. Red contour levels indicate the locations of NH resonances whose $^{1}H/^{15}N$ chemical shift changes as a function of the increasing concentration of L-Trp (from 0.2 to 1.4 mM). The final positions of the $^{1}H/^{15}N$ amide resonances following the addition of 1.6 mM L-Trp are colored blue. The $^{1}H/^{15}N$ chemical shift changes shown are the result of titration of 0.2 mM aliquots of L-Trp into a 1 mM (monomer) WT-TrpR protein solution.

consecutive major grooves of DNA.[5,7] ^{1}H NMR studies have suggested that the DNA-binding region of TrpR retains some degree of flexibility even after L-Trp is bound to the repressor. Flexibility, although incompletely characterized in these studies, is thought to be a critical feature of TrpR that allows the protein to recognize and bind specifically to a wide range of distinct DNA operator sequences.[16]

Mutagenesis experiments have shown that the flexibility and structural ordering of TrpR's DNA-binding domains are affected by slight changes in amino acid composition and lead to altered TrpR functions.[12,17,18] For example, a TrpR variant in which leucine 75 located within the turn of the HTH DNA-binding region is replaced with a phenylalanine (L75F-TrpR) exhibits a unique temperature sensitive (ts) phenotype in which the protein is a more effective repressor at 37 °C than at or above 42 °C.[19] Extensive biochemical characterizations of apo-L75F-TrpR indicated that this function is not due to a poorly structured protein. On the contrary, this TrpR variant exhibits an ∼10% increase in apparent α-helicity as measured by CD, a slightly higher urea denaturation midpoint, and a thermostability (T_m ∼ 90 °C) comparable to that of wild-type TrpR.[19] However, in apo-L75F-TrpR, the HTH DNA-binding domain is disordered (as assessed by a scarcity of intrahelical ^{1}H-^{1}H nOes for this region), suggesting that the helix D−turn−helix E domain of apo-L75F-TrpR is more flexible than the core domain of the protein.[20] Further, comparison of $^{1}H/^{15}N$ HSQC spectra of apo-L75F-TrpR and apo-WT-TrpR recorded under identical conditions revealed significant $^{1}H/^{15}N$ backbone amide chemical shift differences between the two proteins. Changes in $^{1}H/^{15}N$ chemical shifts were observed for amides throughout the protein amino acid sequence and could not be solely rationalized by near-neighbor and ring current effects resulting from the presence of a phenylalanine side chain instead of a leucine side chain at position 75.[20] Interestingly, the three-dimensional (3D) structure of apo-L75F-TrpR did not reveal any significant global overall structural differences between this TrpR variant and apo-WT-TrpR. These findings provided support for the hypothesis that nonlocal long-range effects observed in L75F-TrpR arise from changes in the internal dynamics of the protein rather than being propagated by structural changes.[19]

In contrast to L75F-TrpR, a mutation two residue positions further in the polypeptide chain and within the turn region of the helix D−turn−helix E motif in which alanine 77 is replaced with valine, A77V-TrpR, results in a TrpR variant that exhibits biophysical properties similar to those of L75F-TrpR but different L-Trp and DNA binding functions. A77V-TrpR displays an increase in apparent α-helicity of ∼10% as measured by CD similar to that of L75F-TrpR compared to WT-TrpR, is slightly more stable to urea denaturation than WT-TrpR, and contains a significant number of hydrogen-bonded amide protons that appear to stabilize the structure of the DNA-binding domain of A77V-TrpR.[18,21] DNA binding studies showed that the A77V-TrpR variant has a high affinity for operator DNA in its apo form, an affinity similar in magnitude to the DNA binding affinity of holo-WT-TrpR, but interestingly cannot recognize the full complement of operator sequences normally accessible to

dx.doi.org/10.1021/bi200389k |*Biochemistry* 2011, 50, 5140–5153

WT-TrpR.[12] These results support the notion that the A to V mutation at position 77 results in a more ordered DNA-binding domain in apo-A77V-TrpR and that this structural ordering leads to the restricted specificity of this variant repressor to a subset of DNA sequences.[12,22] This variant was classified as a "super-repressor" because of its ability to repress gene transcription at low L-Trp concentrations relative to those needed for proper functioning of WT-TrpR.[23]

In an attempt to gain further insights into the mechanisms by which subtle changes in amino acid sequence alter protein flexibility with significant effects on TrpR function, we recently reported a detailed analysis of the internal dynamics of backbone amides of WT-TrpR, L75F-TrpR, and A77V-TrpR in their apo (i.e., no L-Trp co-repressor bound) state.[24] In this study, we address the question of to what extent do the two mutations modulate the internal dynamics of the repressors in their L-Trp-bound (holo) forms. That is, does the Leu to Phe mutation preclude L75F-TrpR from achieving a dynamics state that fully matches that of holo-WT-TrpR? Correspondingly, does the Ala to Val mutation permit the HTH region of A77V-TrpR to become more rigid upon corepressor binding, or is the protein already in a "holo" dynamics state in the absence of L-Trp?

We thus have investigated the dynamics of backbone amides of holo-WT-TrpR and two TrpR variants, holo-L75F-TrpR and holo-A77V-TrpR, in their L-Trp-bound (holo) forms using heteronuclear inverse detected two-dimensional (2D) $^{1}H/^{15}N$ solution NMR relaxation experiments. ^{15}N spin−lattice (^{15}N-T_1) and ^{15}N spin−spin (^{15}N-T_2) relaxation time constants and steady-state heteronuclear ^{15}N-$\{^{1}H\}$-nOes were measured for all observable backbone amide ^{15}N nuclei whose NH resonance did not overlap with other NH signals. The ^{15}N NMR relaxation data indicate that all three holo-repressors have comparable internal dynamics profiles with respect to internal NH motions occurring on picosecond to nanosecond time scales, with a few notable and important exceptions for backbone amides within the repressors' HTH DNA-binding domain. Comparing ^{15}N NMR relaxation profiles of the apo- and holo-repressors, we find that L-Trp corepressor binding decreases the amplitude of N−H bond vector fluctuations of backbone amides located in the helix E region of holo-L75F-TrpR and holo-WT-TrpR. A small decrease in flexibility is observed for helix D amides of holo-WT-TrpR, while the flexibility of helix D amides of holo-L75F-TrpR (already motionally restrained to some degree in apo-L75F-TrpR) does not change significantly. Interestingly, backbone amides of holo-A77V-TrpR produce ^{15}N relaxation profiles similar to those observed for apo-A77V-TrpR, indicating that the Ala to Val amino acid substitution at position 77 converts the apo form of this TrpR variant to a repressor form that resembles more closely holo-TrpR in terms of picosecond to nanosecond backbone amide dynamics. This conversion to a holo-TrpR-like protein is independent of whether L-Trp is bound to A77V-TrpR. These observations are consistent with the increased DNA binding affinity and super-repressor phenotype reported for A77V-TrpR.

MATERIALS AND METHODS

Protein Sample Preparations. Engineering of *E. coli* strains CY15071 and CY1575 and the plasmid pJPR2 containing the gene encoding wild-type TrpR (WT-TrpR) or the two variants, L75F-TrpR and A77V-TrpR, have been described previously.[24] Uniformly ^{15}N-labeled or ^{15}N- and ^{13}C-labeled TrpR proteins were isolated from CY15071 or CY15075 cells transformed with their respective plasmids, pJPR2.WT/CY15071, pJPR2.L75F/CY15075, and pJPR2.A77V/CY15071. The strains were grown in M9 minimal medium supplemented with $[^{15}N]NH_4Cl$ (99% ^{15}N-enriched, CIL, Cambridge, MA) or a $[^{15}N]NH_4Cl/[^{13}C_6]$-D-glucose mixture (99% ^{13}C-enriched, CIL) as the sole nitrogen and carbon sources, respectively. Protein purification procedures were conducted as described previously.[19] The CY15071 cell cultures were supplemented with 4 mmol of unlabeled threonine per liter because this strain of *E. coli* cannot synthesize threonine de novo.[25] Thus, TrpR protein samples made from CY15071 bacterial cells lacked ^{15}N-labeled or ^{15}N- and ^{13}C-labeled threonine residues, and as a result, threonine residues from CY15071-derived protein samples could not be observed in 2D or 3D heteronuclear (^{1}H, ^{15}N, and ^{13}C) NMR experiments used for resonance assignments of holo-A77V-TrpR and holo-WT-TrpR, and in the ^{15}N NMR relaxation experiments conducted with these proteins.

NMR Spectroscopy. All multidimensional (^{1}H, ^{15}N, and ^{13}C) NMR spectra were recorded at 318 K (45 °C) on a Bruker DRX 600 MHz NMR spectrometer on samples with protein concentrations ranging from 0.7 to 1.0 mM (subunit) in buffer containing 500 mM NaCl, 50 mM NaH_2PO_4 (pH 5.7), 1 mM NaEDTA, 0.1 mM PMSF, 0.01% (v/v) NaN_3, 5% (v/v) D_2O, and 5 mM L-tryptophan. Two-dimensional gradient-enhanced $^{1}H/^{15}N$ correlation HSQC[26] NMR spectra were recorded with a spectral width of 8012 Hz and 1024 complex points in the ^{1}H (t_2) dimension and a spectral width of 1824 Hz and 256 complex points in the ^{15}N (t_1) dimension. Sequential assignments of ^{1}H, ^{15}N, $^{13}C^{\alpha}$, and $^{13}C^{\beta}$ backbone resonances were made using a standard set of triple-resonance NMR experiments, including HNCACB[27] and CBCA(CO)NH.[28] For all 3D NMR spectra, the data were acquired with spectral widths of 7200 Hz and 1024 complex points (^{1}H t_3 dimension), 1824 Hz and 64 complex points (^{15}N t_1 dimension), and 10000 Hz and 128 complex points (^{13}C t_2 dimension). All NMR spectra were processed using NMRPipe[29] and analyzed using Sparky.[30]

Titration of L-Trp. Titration of L-Trp into apo-TrpR samples was accomplished by adding eight 0.2 molar equivalent aliquots of an L-Trp stock solution [50 mM L-Trp and 50 mM K_2HPO_4 (pH 5.7)] to an ^{15}N-labeled protein solution (1 mM subunit concentration, buffer as described above) of either WT-TrpR, L75F-TrpR, or A77V-TrpR and acquiring the 2D $^{1}H/^{15}N$ HSQC spectrum after each addition to monitor ^{1}H and ^{15}N chemical shift changes upon addition of L-Trp to TrpR samples. Combined ^{15}N and $^{1}H^{N}$ chemical shift changes were calculated by taking into account the gyromagnetic ratios of the ^{15}N and ^{1}H nuclei using the equation $\Delta\delta_{av} = (0.5\{\Delta\delta(^{1}H^{N})^2 + [0.2\Delta\delta(^{15}N)]^2\})^{1/2}$, where $\Delta\delta(^{1}H^{N})$ and $\Delta\delta(^{15}N)$ are the chemical shift differences for the $^{1}H^{N}$ and ^{15}N atoms between holo and apo forms [i.e., $\Delta\delta$ (holo-TrpR − apo-TrpR)], respectively, and $\Delta\delta_{av}$ is a weighted average of the ^{15}N and $^{1}H^{N}$ chemical shifts as described by Pellechia et al.[31] Formation of holo-TrpR samples was considered complete when further addition of L-Trp resulted in no further changes in ^{1}H and ^{15}N chemical shifts as monitored in the 2D $^{1}H/^{15}N$ correlation HSQC spectra of the three holo-repressors.

^{15}N NMR Relaxation Measurements. ^{15}N NMR relaxation experiments, including ^{15}N-T_1, ^{15}N-T_2, and ^{15}N-$\{^{1}H\}$-nOe, were performed at 318 K (45 °C) in triplicate for each holo-TrpR sample using standard NMR relaxation pulse sequences.[32−34] ^{15}N NMR relaxation data were collected for ∼1 mM protein samples (subunit concentration) except for holo-A77V-TrpR whose

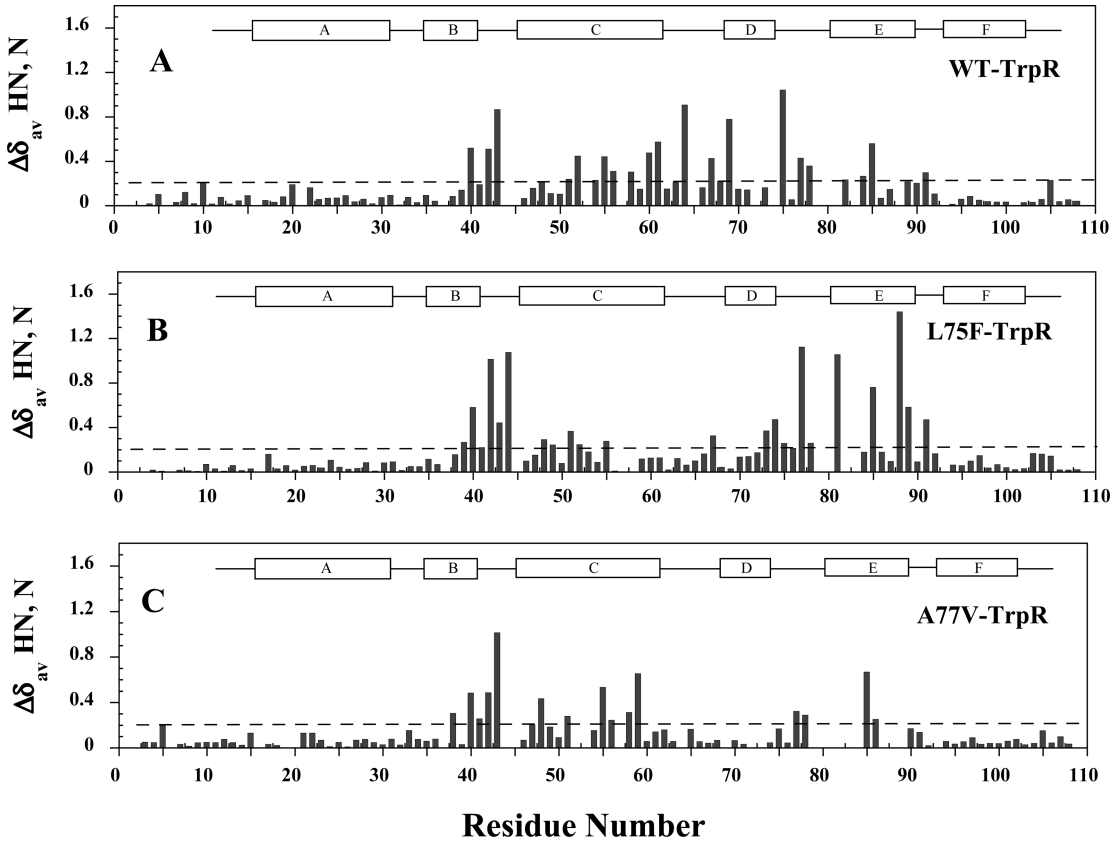

Figure 2. Plots of $^{1}H/^{15}N$ chemical shift changes in TrpR induced by L-tryptophan binding. The chemical shift changes between holo- and apo-TrpR are shown for (A) WT-TrpR, (B) L75F-TrpR, and (C) A77V-TrpR. The reported $\Delta\delta_{av}$ as a function of residue number is a weighted average of the ^{15}N and $^{1}H^{N}$ chemical shifts calculated as follows: $\Delta\delta_{av} = (0.5\{\Delta\delta(^{1}H^{N})^2 + [0.2\Delta\delta(^{15}N)]^2\})^{1/2}$, where $\Delta\delta(^{1}H^{N})$ and $\Delta\delta(^{15}N)$ are the chemical shift differences, i.e., $\Delta\delta$ (holo-TrpR − apo-TrpR), for the $^{1}H^{N}$ and ^{15}N atoms, respectively, between holo and apo forms of the TrpR repressors.

sample concentration ranged from ∼0.65 to 0.70 mM (to minimize the risk of sample aggregation at higher concentrations) in the same sample buffer described above for the preparation of ^{15}N- and ^{13}C-labeled samples used for $^{1}H/^{15}N$ NMR resonance assignments. To verify that sample concentrations were optimal, ^{15}N-T_2 relaxation profiles recorded with lower protein concentrations (∼0.2 and 0.5 mM) were found to be within experimental error no different from the ^{15}N-T_2 profiles measured at ∼1 mM protein (or 0.70 mM for holo-A77V-TrpR), thus ruling out concentration effects.

^{15}N-T_1 and ^{15}N-T_2 experiments were conducted on a Bruker DRX 600 MHz solution NMR spectrometer using proton-detected, sensitivity- and gradient-enhanced inversion-recovery and CPMG pulse sequences for ^{15}N-T_1 and ^{15}N-T_2 data. Spectra were recorded as 1024 × 512 complex points with spectral widths of 7500 and 1824 Hz in the ^{1}H (t_2) and ^{15}N (t_1) dimensions, respectively, using a WALTZ-16[35] ^{15}N-decoupling scheme during the t_2 acquisition time period. The longitudinal relaxation rates (^{15}N-T_1) were determined using inversion-recovery delays of 40, 96, 200, 400, 600, 800, 1000, and 1200 ms. The transverse relaxation rates (^{15}N-T_2) were determined using relaxation delay periods of 8, 16, 32, 40, 64, 80, 104, and 152 ms. ^{15}N-{^{1}H}-nOes were measured using the water-flip-back nOe method and the results corrected for the finite repetition delay according to published protocols.[34] ^{15}N-{^{1}H}-nOe enhancements were determined as the ratio of peak intensities (I/I_o) from NMR data sets acquired with a presaturation pulse and a 4.5 s recycle delay (I) or an off-resonance presaturation pulse and a 4.5 s recycle delay (I_o).[34] ^{15}N-{^{1}H}-nOe spectra were recorded using 1024 and 256 complex data points in the t_2 and t_1 time dimensions of the experiment, respectively, with 48 scans per t_1 increment. To minimize the impact of magnetic field drift, ^{15}N-T_2 and ^{15}N-{^{1}H}-nOe data were collected in an interleaved manner, while 2D ^{15}N-T_1 data sets were acquired consecutively using a list of shuffled relaxation time points. Spectra were processed using NMRPipe,[29] and peak intensities were determined using Sparky.[30] Relaxation rates were determined by nonlinear regression of a two-parameter single-exponential decay equation. Errors in relaxation parameters represent one standard deviation from the mean of replica fits by Sparky. The errors were comparable to those calculated from Monte Carlo calculation[36] or noise standard deviation.

Reduced Spectral Density Mapping. Reduced spectral density analysis was performed using the following relationships as described by Bracken et al.:[37]

$$\sigma_{NH} = R_1(\mathrm{nOe} - 1)\gamma_N/\gamma_H$$

$$J(0.87\omega_H) = 4\sigma_{NH}/(5d^2)$$

$$J(\omega_N) = (4R_1 - 5\sigma_{NH})/(3d^2 + 4c^2)$$

$$J_{eff}(0) = (6R_2 - 3R_1 - 2.72\sigma_{NH})/(3d^2 + 4c^2)$$

where $d = (\mu_o h\gamma_N\gamma_H/8\pi^2)(r^{-3})$ and $c = \omega_N\Delta\sigma/\sqrt{3}$. γ_N and γ_H are the gyromagnetic ratios of the ^{1}H and ^{15}N nuclei, respectively; ω_N and ω_H are the Larmor frequencies; r is the

internuclear $^{1}H-^{15}N$ distance (1.02 Å); $\Delta\sigma$ is the ^{15}N CSA (−160 ppm). The subscript in $J_{eff}(0)$ refers to an "effective" J(0), which is uncorrected for chemical exchange effects.[37,38] Reported error bars were calculated from the propagation of experimental errors determined for the measured ^{15}N-T_1, ^{15}N-T_2, and ^{15}N-$\{^{1}H\}$-nOe series.

ModelFree Analysis. Backbone amide dynamics were characterized by fitting ^{15}N NMR relaxation parameters to one of five semiempirical forms of the spectral density function using the extended model-free formalism described by Lipari and Szabo,[39,40] in a manner analogous to what we have described for the ^{15}N NMR relaxation analysis of backbone amides of the apo-TrpR proteins.[24] Fitting was performed using FAST-ModelFree[41] interfaced with the ModelFree 4.0.1 program.[42] Model selection was based on the statistical testing protocol described by Mandel et al.[43] Initial values of the rotational diffusion tensor for each of the TrpR proteins were estimated from filtered ^{15}N-$T_1/^{15}N$-T_2 ratios using Normadyn[44] and the center of mass-adjusted solution coordinates of holo-TrpR (PDB entry 1WRS). The criteria for including only the core residues in the diffusion tensor estimates were based on the method of Tjandra et al.[45] During ModelFree analysis, the ^{15}N relaxation data were best fitted to an axially symmetric rotational diffusion tensor, with the $^{15}N-^{1}H$ amide bond length assumed to be 1.02 Å and the ^{15}N chemical shift anisotropy estimated to be −160.0 ppm.[46]

RESULTS

^{1}H, ^{15}N, $^{13}C^{\alpha}$, and $^{13}C^{\beta}$ Resonance Assignments of Backbone Atoms. Standard triple-resonance (^{1}H, ^{15}N, and ^{13}C) NMR experiments were used to assign NMR signals from backbone atoms of holo-L75F-TrpR, holo-WT-TrpR, and holo-A77V-TrpR. The HNCACB and CBCA(CO)NH experiments[27,28] permitted identification of $^{13}C^{\alpha}$ and $^{13}C^{\beta}$ resonances and determination of sequential assignments of $^{1}H/^{15}N$ NH resonances (reported in Table S1 of the Supporting Information and BMRB entries 17041, 17046, and 17047). In total, these experiments permitted the assignment of 97 of 104 non-proline backbone residues for holo-WT-TrpR, 102 residues for holo-L75F-TrpR, and 88 residues for holo-A77V-TrpR. As mentioned, because of the fact that the holo-WT-TrpR and holo-A77V-TrpR samples were produced from the CY15071 cell lines, the four threonine residues (Thr 44, Thr 53, Thr 81, and Thr 83) of holo-WT-TrpR and holo-A77V-TrpR were not labeled with ^{15}N and thus precluded their resonance assignments. Other residues that could not be assigned reliably were those with significant NMR resonance overlap or those yielding no signal due to line broadening arising from chemical exchange.

Titration of the L-Trp Corepressor into Apo-TrpR Samples. Backbone amides whose $^{1}H/^{15}N$ chemical shifts changed significantly upon conversion of the TrpR proteins from their apo- to holo-TrpR forms were identified and tabulated. Here, a series of 2D $^{1}H/^{15}N$ HSQC titration experiments were conducted over a range of L-Trp:TrpR molar ratios between 0.2 and 1.6 for the three holo-TrpR repressors. A representative section of overlaid 2D $^{1}H/^{15}N$ correlation HSQC spectra highlighting $^{1}H/^{15}N$ chemical shift changes of several backbone amides of WT-TrpR upon titration of L-Trp is shown in Figure 1B. 2D HSQC spectra of all three TrpR variants containing L-Trp in 1.4−1.6-fold molar excess showed no further spectral changes, indicating that at these L-Trp concentrations, all three repressors have been fully converted to their L-Trp-bound holo states. Chemical shift changes were tabulated by plotting total weighted ^{1}H and ^{15}N chemical shift changes for each residue as described by Pellecchia et al.[31] and are reported in Figure 2. In general, chemical shift changes between holo- and apo-TrpR proteins were found to be small for most amides, indicating that the overall 3D structures of the apo and holo forms of the three TrpR proteins are very similar. However, some residues (~27) exhibited significant $^{1}H/^{15}N$ chemical shift changes upon formation of the holo-repressors. On the basis of $^{1}H/^{15}N$ chemical shift variations, residues with corresponding $\Delta\delta_{av}$ values of ≥0.2 ppm were identified as those experiencing significant chemical shift variations and selected for further analysis. In Figure 1A, residues with significant chemical shift changes are mapped onto the 3D structure of holo-WT-TrpR (PDB entry 1WRS), highlighting that several residues with perturbed chemical shifts clearly cluster around the protein's L-Trp binding pocket. For example, residues 38−44 (the C-terminal end of helix B) and 47−49 (beginning of helix C) point directly at the amino and carboxyl groups of L-Trp. Residues 51, 52, 55, 56, 58, and 59 of helix C and residues 84−86 of helix E are directly adjacent to the L-Trp binding pocket.[6,7] Interestingly, several amides with perturbed chemical shifts belong to residues that are not part of the protein's L-Trp binding pocket. Such amides include residues 60−64 (which comprise the C-terminal end of helix C), residues 67−69 and 73−78 (which span the turn−helix D−turn region of the HTH DNA-binding domain of TrpR), and residues 89−91 of helix E. These data suggest that for these residues, the observed chemical shift changes induced by binding of L-Trp to the repressors originate from indirect effects such as subtle conformational or slow internal dynamics changes.

Not all three TrpR proteins, however, exhibited similar patterns of $^{1}H/^{15}N$ chemical shift changes (Figure 2A−C). For example, WT-TrpR displayed the greatest number of residues with chemical shift changes above the $\Delta\delta_{av} \geq$ 0.2 ppm threshold, with the largest changes occurring for residues located in the turn region spanning helices B and C (i.e., residues 40 and 42−44) and residues in the turn−helix D−turn region (i.e., residues 60, 61, 64, 67, 69, 75, 77, and 78) of TrpR's HTH DNA-binding domain (Figure 2A). L75F-TrpR displayed the second greatest number of residues with chemical shift changes $\Delta\delta_{av}$ of ≥0.2 ppm. The same residues located in the turn region between helices B and C exhibited significantly perturbed $^{1}H/^{15}N$ chemical shifts in L75F-TrpR as in WT-TrpR (Figure 2B). In contrast, a second cluster of residues with large chemical shift changes was localized to the turn−helix E region (residues 77, 81, 85, 88, 89, and 91) of L75F-TrpR, suggesting that the binding of L-Trp to L75F-TrpR causes a change in the chemical environment of helix E, which is not observed in WT-TrpR (Figure 2B). This is in contrast to perturbed residues in the HTH domain of WT-TrpR, which appeared to localize primarily to helix D amides (Figures 1A and 2A).

Lastly, A77V-TrpR displayed the lowest number of amide residues with chemical shift changes ($\Delta\delta_{av}$) of ≥0.2 ppm. Residues with significant $^{1}H/^{15}N$ chemical shift changes were located at the end of helices B, C, and E, similar to what was observed for WT-TrpR, and spanning the L-Trp binding pocket of the repressor. The largest differences between A77V- and WT-TrpR were found for residues in the turn−helix D−turn region. A77V-TrpR had very few residues in this region with perturbed $^{1}H/^{15}N$ chemical shifts compared to wild-type TrpR (Figure 2C). Overall, these data indicated that the chemical shift changes observed upon formation of holo-A77V-TrpR are

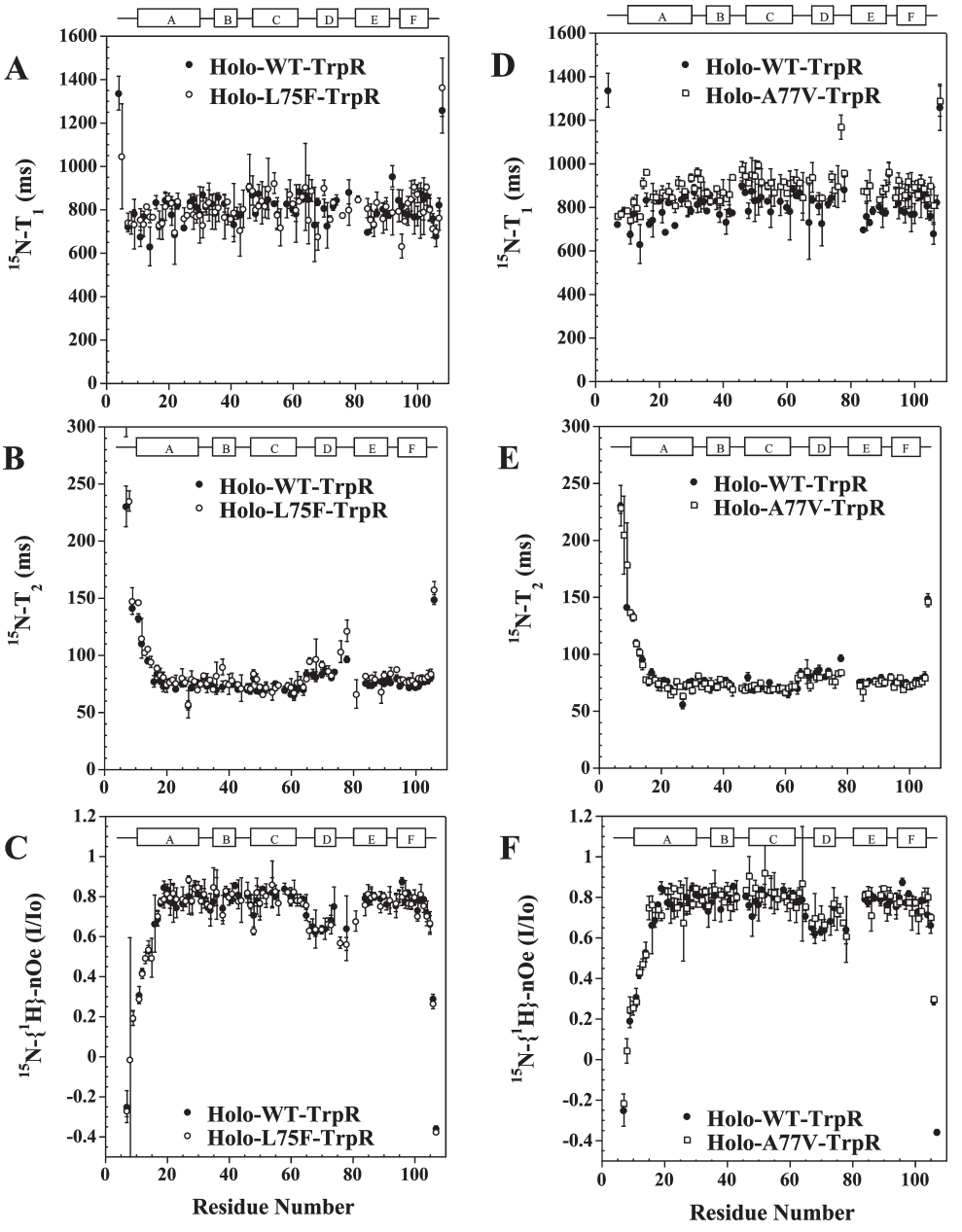

Figure 3. Comparison of ^{15}N NMR relaxation parameters as a function of residue number for holo-L75F-TrpR (right column, ○) and holo-A77V-TrpR (left column, ○): (A) ^{15}N-T_1, (B) ^{15}N-T_2, and (C) ^{15}N-{^{1}H}-nOe recorded at a static magnetic field strength of 14.1 T (i.e., 600 MHz ^{1}H Larmor frequency). The corresponding data for holo-WT-TrpR (●) are shown in each plot for direct comparison. Secondary structural elements of TrpR are depicted above each plot.

almost exclusively associated with residues lining the L-Trp binding pocket of the repressor. The absence of significant ^{1}H/^{15}N chemical shift changes for residues in the helix D−turn−helix E (HTH) region of A77V-TrpR suggests that the conformation of A77V-TrpR in its apo state closely mimics that of the L-Trp-bound holo form of the protein.

Further, a comparison of the overlaid 2D ^{1}H/^{15}N HSQC spectra of the L-Trp-saturated forms of holo-WT-TrpR and holo-A77V-TrpR revealed an interesting trend and indicated that ∼98% of the ^{1}H/^{15}N chemical shifts are identical for holo-WT and holo-A77V TrpR. Any observed chemical shift differences for the two holoproteins corresponded to resonances in holo-A77V-TrpR that are marginally offset in terms of chemical shifts relative to corresponding signals of holo-WT-TrpR. The close resemblance of spectral patterns in the 2D ^{1}H/^{15}N HSQC spectra of the two holo-repressors suggests that the conformations of their L-Trp-bound state are almost identical. This is not the case for holo-L75F-TrpR where only ∼91% of the observed NH signals overlaid directly with those of holo-WT-TrpR in 2D ^{1}H/^{15}N HSQC spectra of these proteins recorded under identical conditions. The remaining ∼9% (∼9 residues) exhibited small but distinct chemical shift differences from corresponding NH signals of holo-WT-TrpR. These differences were assigned to amides in the HTH domain of TrpR within the stretch of residues 61−79 and amides located in turn regions spanning helix D and next to helix E (i.e., residues 60, 64, 67, 76,

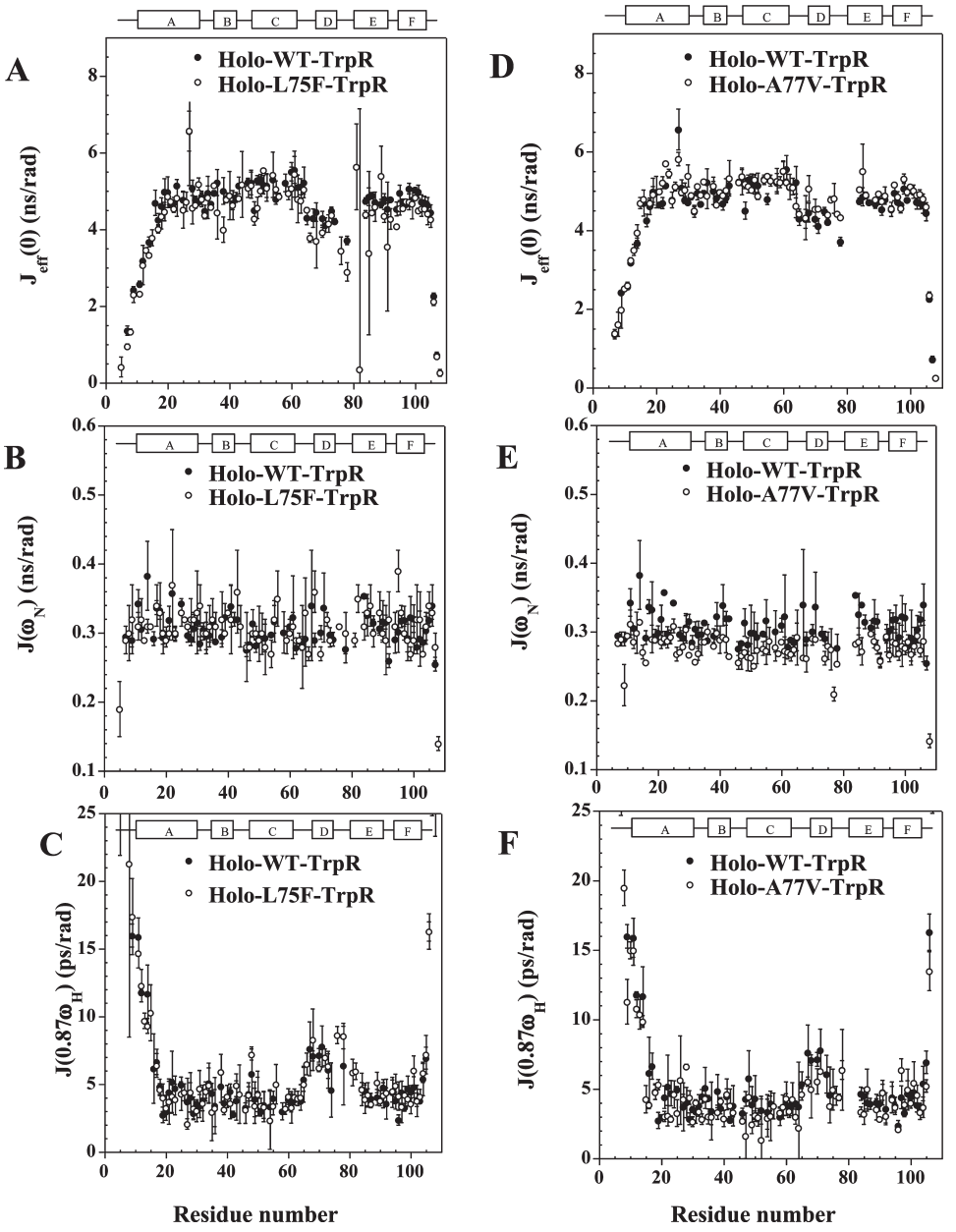

Figure 4. Comparison of reduced spectral density functions calculated for holo-L75F-TrpR (left column, ○) and holo-A77V-TrpR (right column, ○): (A) $J_{eff}(0)$, (B) $J(\omega_N)$, and (C) $J(0.87\omega_H)$. The corresponding data for holo-WT-TrpR (●) are shown in each plot for direct comparison. The positions of secondary structural elements in the amino acid sequence of TrpR are shown above each plot as a function of residue number.

78, 89, and 91). Distinct chemical shifts would be expected for residues close to Phe 75 due to potential ring current effects introduced by the Leu to Phe amino acid substitution in L75F-TrpR. Others are too distant to be experiencing substantial ring current effects, and their distinct chemical shifts most likely originate from small conformational and/or dynamics changes within helices C, D, or E that propagate outward to adjacent turn regions.

Interestingly, small differences in chemical shifts between holo-WT-TrpR and holo-L75F-TrpR were observed for residues located in the C-terminal ends of helices C and E (i.e., residues 56, 60, 89, and 90), consistent with previously observed differences in $^1H/^{15}N$ chemical shifts between the 2D $^1H/^{15}N$ spectra of apo-L75F-TrpR and apo-WT-TrpR.[20] On the basis of these data, we thus conclude that the long-range perturbations observed in apo-L75F-TrpR persist in holo-L75F-TrpR.

^{15}N NMR Relaxation Measurements. ^{15}N-T_1, ^{15}N-T_2, and ^{15}N-$\{^1H\}$-nOe were determined for 76, 80, and 78 of 108 backbone amides of holo-WT-TrpR, holo-L75F-TrpR, and holo-A77V-TrpR, respectively, at a static magnetic field strength of 600 MHz (^1H Larmor frequency). The following residues were excluded from the analysis: four prolines, unlabeled threonine resonances, and resonances in which spectral overlap precluded accurate determination of peak intensities as required for reliable analysis of ^{15}N NMR relaxation data. Measured ^{15}N-T_1, ^{15}N-T_2, and ^{15}N-$\{^1H\}$-nOe values for backbone amides of holo-WT-TrpR, holo-L75F-TrpR, and holo-A77V-TrpR are shown in Figure 3. To highlight similarities and differences

between data sets, we plotted the ^{15}N NMR relaxation data of holo-L75F-TrpR and holo-A77V-TrpR in comparison with those of holo-WT-TrpR. A complete listing of all ^{15}N NMR relaxation parameters measured for all three holo-TrpR proteins is included in the supplementary tables included in the Supporting Information and reported in the BMRB (entries 17041, 17046, and 17047).

As shown in Figure 3A, the ^{15}N-T_1 profile for holo-WT-TrpR is quite uniform, averaging to an ^{15}N-T_1 value of 807 ± 50 ms, with the exception of large ^{15}N-T_1 values (>1000 ms) measured for backbone amides located in the N- and C-terminal ends of the protein. ^{15}N-T_1 profiles for holo-L75F-TrpR and holo-A77V-TrpR (Figure 3A,D) are also quite uniform, averaging to 802 ± 62 and 889 ± 43 ms, respectively. These ^{15}N-T_1 relaxation values are consistent with the 25 kDa molecular weight of the TrpR repressors and comparable to what has been reported for WT-TrpR.[15]

Measured ^{15}N-T_2 values as a function of residue number are plotted in panels B and E of Figure 3. For all three holo-repressors, large ^{15}N-T_2 values (>100 ms) were measured for backbone amides located in the N- and C-termini of the proteins (residues 4−14 and 106−108). Backbone amides located in core α-helices A−C and F (i.e., residues 16−32, 35−42, 45−63, and 93−108, respectively) of the three holo-repressors yielded rather uniform ^{15}N-T_2 values, averaging to 75 ± 5, 77 ± 8, and 73 ± 4 ms for holo-WT-TrpR, holo-L75F-TrpR, and holo-A77V-TrpR, respectively. Interestingly, a break in the uniformity of the ^{15}N-T_2 profiles was observed for all three holoproteins starting at residue E65 and ending at R84 (Figure 3B and 3E). This region corresponds to the turn−helix D−turn−helix E DNA-binding domain of the repressors. The ^{15}N-T_2 profiles of holo-WT-TrpR and holo-A77V-TrpR in this region (Figure 3E) were almost identical. ^{15}N-T_2 values for holo-L75F-TrpR amides followed, for the most part, trends similar to those of holo-WT-TrpR and holo-A77V-TrpR, with the exception of two amides (G76 and G78) that displayed significantly higher ^{15}N-T_2 values, suggesting that these two residues are significantly more flexible in L75F-TrpR than in the two other TrpR variants. These two glycines are located in the turn region of the HTH DNA-binding domain next to the amino acid substitution site and may be at the source of the flexibility differences observed for helix D amides of holo-L75F-TrpR (see below).

The ^{15}N-{^{1}H}-nOe profiles of backbone amides of holo-WT-TrpR and the two TrpR variants are shown in panels C and F of Figure 3. Large decreases in ^{15}N-{^{1}H}-nOe (<0.6) were observed for backbone amides in the N- and C-termini of the holo-repressors (residues 4−15 and 105−108, respectively). These measured ^{15}N-{^{1}H}-nOes, together with the large ^{15}N-T_1 and ^{15}N-T_2 values measured for these amides, clearly indicated that the backbone amides located at the ends of the holo-TrpR proteins undergo large amplitude picosecond to nanosecond motions. ^{15}N-{^{1}H}-nOes for backbone amides in the core helices were quite uniform, averaging to 0.78 ± 0.06, for all three holo-repressors, indicating that core amides are motionally restricted in terms of picosecond to nanosecond fluctuations and are part of a rigid structural core for all three TrpR proteins. In contrast, ^{15}N-{^{1}H}-nOes for residues located at the end of helix C (starting at residue E65) and progressing toward the beginning of helix E (residue A80) decreased for all three holo-repressors (see Figure 3C and 3F and Supporting Information). Some of the lowest ^{15}N-{^{1}H}-nOes were measured for backbone amides preceding and directly following helix D (i.e., turn residues) as well as in helix D (e.g., M66, Q68, E70, L71, G76, and G78). This observed decrease in ^{15}N-{^{1}H}-nOe correlates well with the slight elevation in ^{15}N-T_2 observed for these residues (Figure 3B and 3E). Overall, ^{15}N-T_1, ^{15}N-T_2, and ^{15}N-{^{1}H}-nOes measured for holo-WT-TrpR, holo-L75F-TrpR, and holo-A77V-TrpR are largely within experimental error of each other, indicating that all three holo-repressors have overall very similar ^{15}N NMR relaxation behaviors, except for a few important residues within or in the vicinity of the repressors' HTH DNA-binding domain.

Reduced Spectral Density Mapping. The ^{15}N NMR relaxation data for all three holo-repressors were analyzed in terms of reduced spectral density functions [$J_{eff}(0)$, $J(\omega_N)$, and $J(0.87\omega_H)$], as this approach has the advantage in that these functions are sensitive to frequencies of motions rather than amplitudes of motions and less prone to limitations of model fitting.[37,47,48] A plot of the three reduced spectral density functions as a function of residue number is shown in Figure 4A−F for the three holo-TrpR repressors, and a complete tabulation of results is available in the Supporting Information (Tables S5−S7).

Consistent with ^{15}N-T_1, ^{15}N-T_2, and ^{15}N-{^{1}H} -nOe trends, the reduced spectral density functions $J_{eff}(0)$, $J(\omega_N)$, and $J(0.87\omega_H)$ are quite uniform for N−H bond vectors of core amides residing in α-helices A−C and F of all three holo-repressors and for helix E amides. This indicates that the internal picosecond to nanosecond dynamics of N−H bond vectors in these regions of the proteins are comparable. $J(\omega_N)$ functions were very similar throughout the sequence of all three proteins (see Figure 4B and 4E). Uniformity in the $J(\omega_N)$ patterns is consistent with the uniform trends observed in the ^{15}N-T_1 data, reflecting the same insensitivity to residue position and is not too surprising considering that $J(\omega_N)$ is a measure of the spectral power of frequencies that contribute significantly to ^{15}N-T_1 relaxation.[37] Using reduced spectral density functions for core residues, an apparent correlation time (τ_m) for overall reorientation of the holo-repressors in solution was calculated using the following equation:[37]

$$\tau_m = \omega_N^{-1}\{[J_{eff}(0) - J(\omega_N)]/J(\omega_N)\}^{1/2}$$

and yielded τ_m values of 10.12 ns for holo-L75F-TrpR, 10.38 ns for holo-WT-TrpR, and 11.03 ns for holo-A77V-TrpR.

In contrast to spectral density functions calculated for amides of the core helices, small $J_{eff}(0)$ and large $J(0.87\omega_H)$ values were observed for amides residing in the N- and C-terminal ends of the three proteins. These data are consistent with ^{15}N-T_1, ^{15}N-T_2, and ^{15}N-{^{1}H}-nOe trends indicating that the disordered N- and C-terminal segments of TrpR experience rapid and large amplitude picosecond to nanosecond internal motions.

Differences in $J_{eff}(0)$ and $J(0.87\omega_H)$ values were also observed for backbone amides located within the turn−helix D−turn segment of the HTH DNA-binding domain of the three holo-repressors. $J(0.87\omega_H)$ increased by ∼4.0 ps/rad and $J_{eff}(0)$ decreased by ∼0.8 ns/rad compared to the $J(0.87\omega_H)$ and $J_{eff}(0)$ of core and helix E amides. These trends in reduced spectral density functions indicated that helix D amides of all three holo-repressors experience a greater degree of picosecond to nanosecond internal fluctuations than amides in the core α-helices and in helix E. Further, although subtle, we observed that the internal dynamics of helix D amides of holo-A77V-TrpR were slightly reduced compared to those of holo-WT-TrpR (Figure 4F).

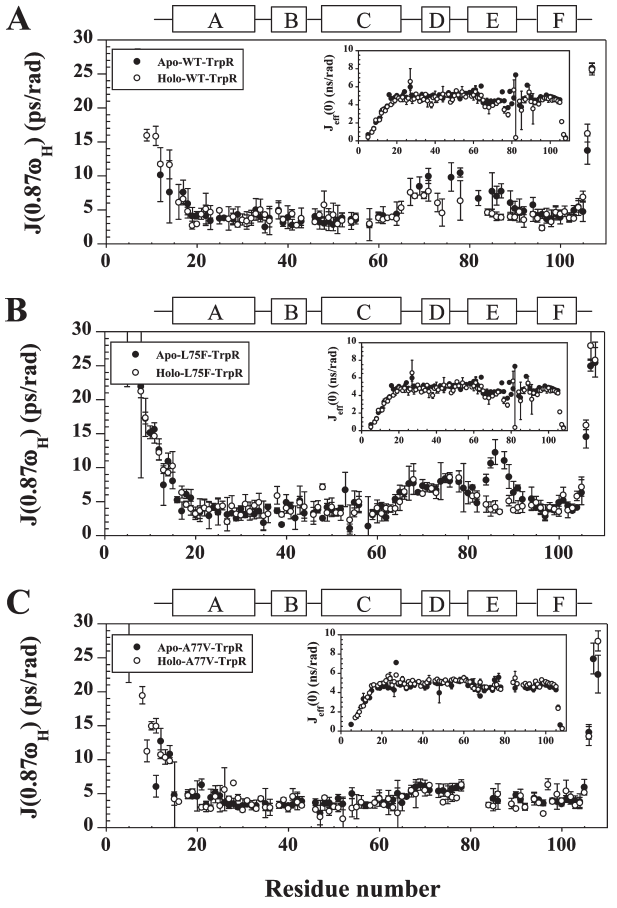

Figure 5. Comparison of reduced spectral density functions $J(0.87\omega_H)$ and $J_{eff}(0)$ (insets) calculated for apo (●) and holo (○) forms of WT-TrpR (A), L75F-TrpR (B), and A77V-TrpR (C), with schematics of secondary structural elements of TrpR depicted above the plots.

ModelFree Analysis of ^{15}N NMR Relaxation Parameters: ^{15}N NMR relaxation parameters of holo-WT-TrpR, holo-L75F-TrpR, and holo-A77V-TrpR were also analyzed using ModelFree and the model selection approach of Mandel and co-workers.[43] This approach provides a different set of parameters (namely S^2 and model selection), which is also useful for characterizing internal dynamics in proteins based on ^{15}N NMR relaxation data. Details of the ModelFree analysis are included as Supporting Information and support the internal flexibility trends deduced from the reduced spectral density function analysis.

Comparison of the Internal Backbone Amide Dynamics of the Holo-Repressors to Those of the Apo-TrpR Proteins. The NH backbone dynamics profiles of holo-WT-TrpR, holo-L75F-TrpR, and holo-A77V-TrpR were analyzed in the context of detailed ^{15}N NMR relaxation data recently measured for the corresponding apo-repressors.[24] Comparative $J(0.87\omega_H)$ and $J_{eff}(0)$ profiles are shown in Figure 5 as a function of residue number. These comparisons highlight the most notable backbone dynamics changes occurring upon L-Trp co-repressor binding and the effects that the Leu to Phe and Ala to Val mutations at positions 75 and 77, respectively, impart on the transition from apo- to holo-repressor. Comparison of $J(\omega_N)$ profiles (data not shown) between the apo and holo forms of all three proteins revealed no significant differences between the apo and holo states, consistent with uniform ^{15}N-T_1 trends observed for all apo- and holo-TrpR proteins. In contrast, comparison of the $J(0.87\omega_H)$ profiles highlighted significant protein-specific differences. For WT-TrpR, the $J(0.87\omega_H)$ profiles between the apo and holo forms of the repressor were very similar for backbone amides located in the core α-helices of the protein but were noticeably higher for amides located within the helix D−turn−helix E DNA-binding domain of apo-WT-TrpR (Figure 5A). This difference was also observed in the lower S^2 order parameters calculated for these residues in the apo-repressor state (see Supporting Information). Thus, it is clear that binding of L-Trp co-repressor to apo-WT-TrpR reduces the internal dynamics of amides within the helix D−turn−helix E region of the repressor. This "stiffening" of the HTH DNA-binding domain of WT-TrpR as observed in these ^{15}N NMR relaxations studies is consistent with the sequential stabilization model of helices E and D upon L-Trp and DNA binding, respectively.[9,16]

In the case of L75F-TrpR, backbone amides located within the core α-helices of the repressor displayed comparable $J(0.87\omega_H)$ profiles upon comparison of the apo-repressor and L-Trp-bound holo-repressor states. Similarly, no significant changes in $J(0.87\omega_H)$ profiles were observed for helix D amides in the two protein states (Figure 5B), indicating that the relative stiffening of helix D observed in apo-L75F-TrpR (but not in apo-WT-TrpR)[24] is not further stabilized or enhanced by L-Trp binding. In contrast, backbone amides in helix E exhibited a drastic change in $J(0.87\omega_H)$ profiles between the apo and holo states of L75F-TrpR (Figure 5B). $J(0.87\omega_H)$ values measured for residues 84−89 were significantly lower in apo-L75F-TrpR. Upon formation of the holo-repressor, $J(0.87\omega_H)$ values for these residues decreased significantly, converging to a uniform value of ∼4 ps/rad, indicating that upon formation of holo-L75F-TrpR picosecond to nanosecond motions experienced by helix E amides become significantly restricted, rendering these amides almost as rigid as amides in the core α-helices. Interestingly, S^2 values calculated for amides in the helix D−helix E region of the apo and holo forms of L75F-TrpR were found to be quite similar. However, upon examination of the model selection best fit for helix E, one can see that in the apo form several residues were best fit with models 5 and 4, indicating very complicated motions that cannot be well parametrized using the ModelFree formalism, whereas in the holo form of L75F-TrpR, many of these same residues were now amenable to ModelFree parametrization and best fit to simpler models of motions, i.e., model 1 or 2, where ModelFree analysis is most interpretable (see Supporting Information). This change in model selection is consistent with amides in the HTH domain of L75F-TrpR becoming less flexible and experiencing less complicated motions upon formation of holo-L75F-TrpR. Overall, the ^{15}N NMR relaxation data collected for apo- and holo-L75F-TrpR indicated that the Leu to Phe amino acid substitution at position 75 imparts greater flexibility to helix E of apo-L75F-TrpR compared to that of apo-WT-TrpR, and that upon L-Trp binding, the flexibility seen in helix E of apo-L75F-TrpR is significantly reduced, rendering helix E almost as rigid as core α-helices.

In contrast to the reduced spectral density patterns observed for L75F-TrpR, $J(0.87\omega_H)$ and $J_{eff}(0)$ measured for backbone amides of apo- and holo-A77V-TrpR are very similar, including those of amides residing in the HTH DNA-binding domain of the protein (Figure 5C). These data indicate that the backbone flexibility of apo- and holo-A77V repressors is comparable and that both proteins are more rigid than either WT- or L75F-TrpR.

These data also suggest that the apo state of A77V-TrpR already populates a set of conformations that mimic the predominant conformation of the holo-repressor.

Further, examination of S^2 generalized order parameters as a function of residue number revealed no significant difference between apo- and holo-A77V-TrpR, consistent with reduced spectral density function analyses (see Supporting Information). The S^2 trends pointed to a rigid protein core with a slightly greater degree of picosecond to nanosecond internal motion in the helix D−turn region, and a rigid helix E domain. Altogether, the data suggest that the backbone amide dynamics of apo- and holo-A77V-TrpR are similar, allowing us to corroborate that the Ala to Val amino acid substitution at position 77 causes the resulting TrpR variant to adopt dynamics features of the L-Trp corepressor bound (holo) form even in the absence of L-Trp corepressor.

Analysis of Backbone Amide Dynamics of L-Trp Ligand-Binding Specific Residues (apo- vs holo-TrpR). Because L-Trp binding is known to induce a specific structural change in the TrpR protein,[5,6,9] we investigated whether residues that are influenced by L-Trp binding (i.e., amides that undergo significant $^1H/^{15}N$ chemical shift changes upon the transition from the apo to the holo states of TrpR) also undergo significant backbone amide dynamics changes. Analysis of ^{15}N NMR relaxation profiles, S^2, and spectral density functions revealed that little correlation exists between residues experiencing large $^1H/^{15}N$ chemical shift changes upon L-Trp binding to the repressors (Figure 2) and those with significant changes in backbone amide dynamics between the apo and holo forms of the TrpR proteins (Figure 5A−C). The low correlation is likely a reflection of the fact that chemical shift changes can result from a variety of factors, including small conformational changes such as changes in dihedral angles, side chain χ angles, hydrogen bond interactions, local electric fields, proximity and orientation of aromatic rings, e.g., the binding of L-Trp, ionization and oxidation states, and backbone dynamics. Further, it should be noted that chemical shift changes report on structural and/or dynamics processes occurring on a slower (millisecond) time scale, whereas the ^{15}N NMR backbone amide relaxation experiments reported here are sensitive to dynamics processes occurring on much faster picosecond to nanosecond time scales.

DISCUSSION

While characterization of protein conformational changes induced by ligand binding can be accomplished relatively easily through detailed structural analyses, dynamics changes modulating the ligand binding properties of proteins are more subtle and difficult to monitor experimentally. NMR spectroscopy is well suited to determine both structural and flexibility changes at atomic-level resolution[49,50] and provides quantitative information about protein conformational dynamics.[51,52] In this work, we have measured and analyzed the $^{15}N/^1H$ backbone amide dynamics properties of the tryptophan repressor (WT-TrpR) and two TrpR variants with distinct phenotypes: L75F-TrpR (i.e., a temperature sensitive variant) and A77V-TrpR (i.e., a super-repressor variant) in their L-Trp-bound (holo) state. Analysis of the ^{15}N NMR relaxation data indicates that the backbone amide dynamics profiles of the holo-repressors are comparable. Thus, the individual L75F and A77V amino acid substitutions do not impact the holo-repressor states as much as that of the apo-repressors.[20] Backbone amide dynamics for the three holo-TrpR repressors can be summarized as follows. (1) The N-terminal and C-terminal ends of the proteins (residues 4−14 and 106−108, respectively) experience significant picosecond to nanosecond backbone amide motions and low S^2 values reflecting the extensive flexibility of the N- and C-termini of all three TrpR proteins. (2) Backbone amides located within α-helices A−C and F that form the core of the TrpR dimer are characterized by limited picosecond to nanosecond N−H bond vector motions and high S^2 values indicating that picoseconed to nanosecond internal motions of core amides are restricted significantly. (3) Backbone amides located in helix E of the HTH DNA-binding domain of the holo-repressors exhibit comparable restrictions in picosecond to nanosecond motions and high S^2 values compared to those calculated for backbone amides in the core α-helices, demonstrating that the internal flexibility of helix E amides is as limited as that of core amides. (4) Helix D amides of holo-L75F-TrpR, which were shown to be less flexible in apo-L75F-TrpR than corresponding amides in apo-WT-TrpR, are unaffected by L-Trp binding and continue to retain the same degree of limited flexibility compared to what is observed for amides in core helices. In contrast, helix D amides of holo-WT-TrpR undergo a small but significant "stiffening" and a corresponding decrease in picosecond to nanosecond N−H bond vector fluctuations. Helix D amides of holo-A77V-TrpR, which were rigid in apo-A77V-TrpR, remain motionally restricted in holo-A77V-TrpR.

Extensive biochemical experiments with WT-TrpR suggested that the primary effect of L-Trp binding on the repressor is to stabilize helix E, the recognition helix of the helix D−turn−helix E (HTH) DNA-binding domain, subsequently permitting optimal interaction with DNA operator sequences.[5,7,14] The ^{15}N NMR relaxation studies presented herein support such a hypothesis and highlight subtle but important changes in backbone amide dynamics occurring within or in the vicinity of the HTH domain of TrpR as a result of the Leu to Phe and Ala to Val amino acid substitutions at positions 75 and 77, respectively.

Quite surprisingly, in the case of L75F-TrpR, the mutation clearly causes a significant increase in the flexibility of backbone amides located in the N-terminus of helix E of apo-L75F-TrpR,[24] which is significantly reduced upon formation of holo-L75F-TrpR (Figure 5B). One would have anticipated that the Leu to Phe amino acid substitution (located at the very C-terminal end of helix D) would perturb to a greater extent the flexibility of helix D amides upon formation of the holo-repressor. On the contrary, we observed that the internal flexibility of helix D amides decreased in apo-L75F-TrpR compared to its flexibility in apo-WT-TrpR[24] and did not change upon formation of holo-L75F-TrpR. These dynamics data are consistent with structural information about apo-L75F-TrpR that revealed that although helices D and E of the apo-repressor are less well-defined than core helices in the 3D structure of apo-L75F-TrpR, a greater α-helical propensity was noted for helix D residues as inferred from the presence of additional ^1H-^1H nOes in this region[20] compared to what was observed in apo-WT-TrpR.[22]

Binding studies have shown that the L75F-TrpR variant has a 10-fold lower L-Trp binding affinity than WT-TrpR.[19] Our data suggest that the greater picosecond to nanosecond internal motions of helix E and the "stiffening" of helix D of apo-L75F-TrpR contribute to the lower ligand binding affinity of this ts TrpR variant. We postulate that the enhanced flexibility of helix E in apo-L75F-TrpR translates into molecular perturbations around the L-Trp binding pocket of the repressor. This is consistent with the fact that several helix E amides that

experience significant $^{1}H/^{15}N$ dynamics changes upon L-Trp binding are also involved with the formation of specific ligand binding interactions with the L-Trp corepressor. Similarly, we suspect that the "stiffer" helix D in apo-L75F-TrpR generates an energy barrier for the ordering of helix E upon L-Trp binding and formation of holo-L75F-TrpR.

In contrast to L75F-TrpR, the A77V-TrpR variant is already rather rigid as an apo-repressor,[24] and no significant changes in the picosecond to nanosecond internal dynamics for helix E amides take place upon formation of holo-A77V-TrpR. L-Trp binding thus does not trigger a further rigidification of the protein, and helix E stays as rigid as it was in apo-A77V-TrpR. From these data, we conclude that the Ala to Val substitution at position 77 has the effect of converting the variant apo-repressor into a holo-repressor-like state. Interestingly, despite observing significant $^{1}H/^{15}N$ chemical shift changes in the 2D $^{1}H/^{15}N$ correlation HSQC spectra of A77V-TrpR upon L-Trp binding, no significant picosecond to nanosecond backbone dynamics changes seem to be taking place in the variant holo-repressor. Our data support a model in which the primary effect of L-Trp co-repressor binding to TrpR is to contribute to the formation of a well-ordered helix E. In the case of A77V-TrpR, the resulting amino acid substitution triggers such ordering of helix E and co-repressor binding has little effect on this conformational transition. Our ^{15}N NMR relaxation observations are consistent with a model in which the reduced flexibility of helix E contributes to the weakened ability of A77V-TrpR to distinguish between closely related DNA operator sequences.[22]

In contrast to helix E, our ^{15}N NMR relaxation data on all three holo-repressors indicate that the flexibility of helix D amides is not significantly affected by L-Trp binding and retains a certain degree of picosecond to nanosecond internal motions, although the extent of flexibility differs among the three proteins. These data provide additional support for a sequential ordering model of the helix D−turn−helix E region upon L-Trp and DNA binding to the repressor.[16] They also support the notion that residual flexibility in TrpR is essential for repressor function, DNA binding, and molecular recognition of target operators.

The overall picture that emerges is that although all three holo-repressors display comparable picosecond to nanosecond internal fluctuations for many amides in the core and DNA-binding domain of the holo-repressors, several differences in internal dynamics are observed upon transition from the apo- to the holo-repressors. These differences are most pronounced for residues in the HTH DNA-binding domains of L75F- and WT-TrpR. In contrast, the backbone amide dynamics profiles of A77V-TrpR in its apo and holo forms are very similar, including the HTH residues. It is interesting to note that despite the fact that the two TrpR variants share many characteristics such as the proximity of the mutation sites (positions 75 and 77 in the polypeptide sequence), similar amino acid properties (i.e., both hydrophobic residues), and comparable CD and thermal stability profiles, these mutations have distinct and profound impacts on the internal dynamics of these proteins. In the case of L75F-TrpR, the replacement of Leu 75 with Phe results in the increased flexibility of helix E and a stiffening of helix D amides, whereas the substitution of Ala 77 for Val in A77V-TrpR decreases the motional flexibility of helix E and helix D amides. The differences in internal motions that we have observed correlate well with extensive structural studies of TrpR variants and reinforce the close relationship between structure and dynamics. They also provide evidence that changes in protein flexibility play an important role and contribute significantly to the altered L-Trp binding affinity, distinct DNA binding affinity, and phenotypic properties of the three proteins.

TrpR Flexibility in the Context of the Functions of Other DNA-Binding Proteins. Recent dynamics studies of other DNA- and ligand-binding proteins reveal features similar to those of TrpR. For example, a comparison of the backbone amide dynamics of apo- and holo-cellular retinol-binding protein by Franzoni et al.[53] demonstrated that a reduction in protein flexibility takes place upon transition of the protein from the apo to the holo state. Further, these authors suggested that the flexibility in the apo-state may assist in ligand uptake, while the "stiffening" of the backbone in the holo-protein guarantees the stability of the complex for subsequent function, a model that can be easily applied to TrpR. In addition, Zhu et al.,[54] investigating the dynamics of the Mrf-2 DNA-binding domain free and in complex with DNA, showed that it is the two flexible interhelical loops, the flexible C-terminal tail, and one α-helix that are involved in DNA recognition. This is similar to the case for TrpR in which the most flexible part of the protein is the DNA-binding interaction site. Further, these authors continued to observe picosecond to nanosecond and slower microsecond to millisecond time scale motions at the DNA-bound surface of Mrf-2, suggesting a model where interactions between the DNA and the protein remain highly dynamic. Earlier studies on the dynamics of TrpR with DNA also showed that although the helix D region becomes stiffer, a certain degree of flexibility remains.

Two other studies, one by Dangi et al.[55] investigating the dynamics of MarA−DNA complexes and the second by Brown et al.[56] investigating how protein flexibility directs DNA recognition by the papillomavirus E2 protein, indicated that flexibility is required for binding different DNA sequences (i.e., both non-specific and specific DNA binding can be enhanced by altering interdomain flexibility). These results lead to the conclusion that a reduced level of protein movement would be expected to diminish the fine-tuning of complementarity and impart an entropic cost to the interaction, thereby weakening binding for some degenerate consensus sequences, similar to what is observed for A77V-TrpR.

Studies of the lactose repressor (LacI),[57] another DNA-binding protein, reveal that protein flexibility plays a significant role in modulating the allosteric response of the repressor, its oligomerization state, small molecule binding, and protein-protein interactions.[58,59] Remarkably and as for TrpR, amino acid substitution of residues in LacI located in a solvent-exposed flexible loop that is crucial for function results in altered inducer and DNA operator binding properties, and two mutations that are close in sequence (i.e., L148F and S151P) result in opposite changes in operator/inducer binding affinities in the LacI variants.[57,58] These elegant studies have shown that residues in this flexible loop (i.e., LacI residues 149−156) make important contributions to the allosteric regulation of the repressor, which we find to be very similar to what is observed for TrpR.

In the case of the *E. coli* cytidine repressor (CytR), Senear and co-workers have shown that protein flexibility plays an important role in the adaptability of the repressor to bind to different operators of varying spacer lengths, and while CytR is structurally well-ordered in solution, it is also highly flexible.[60,61] Interestingly, these studies have also suggested that the DNA-binding domain of CytR can adopt various DNA-bound conformations, some more rigid than others.[61] Residual flexibility of the CytR

DNA-binding domain is reminiscent of the intrinsic flexibility observed in the HTH DNA-binding domain of TrpR.

In summary, it is clear that protein flexibility is important for DNA binding and molecular recognition of target operators for a large family of DNA-binding proteins.[61−63] However, detailed studies are needed to tease out the mechanisms by which protein dynamics specifically influence function in any given protein−DNA system. It is interesting to note, however, that key residues are often found on solvent-exposed flexible loops, reinforcing the concept that protein motions are important for molecular recognition. It is also expected that the internal motions of side chain atoms would be crucial for the modulation of the allosteric responses of DNA-binding proteins. Side chain dynamics studies have not been conducted on TrpR variants but are certainly worth considering for future studies.

■ ASSOCIATED CONTENT

Supporting Information. A detailed text description of the ModelFree analysis of ^{15}N NMR relaxation parameters for holo-WT-TrpR, holo-L75F-TrpR, and holo-A77V-TrpR and Tables S1−S10. This material is available free of charge via the Internet at http://pubs.acs.org.

Accession Codes

^{15}N, ^{1}H, and ^{13}C chemical shift data, ^{15}N NMR relaxation data, spectral density, and ModelFree parameters characterizing backbone amide dynamics have been deposited in the Biological Magnetic Resonance Data Bank as entries 17041, 17046, and 17047 for holo-WT-TrpR, holo-L75F-TrpR, and holo-A77V-TrpR, respectively.

■ AUTHOR INFORMATION

Corresponding Author

*Department of Chemistry and Biochemistry, Montana State University, P.O. Box 173400, Bozeman, MT 59717. E-mail: vcopie@chemistry.montana.edu. Phone: (406) 994-7244. Fax: (406) 994-5407.

Funding Sources

This work has been supported by National Science Foundation Grant MCB-0444056.

■ ACKNOWLEDGMENT

The NMR experiments were conducted at Montana State University on a Bruker DRX600 NMR spectrometer purchased in part with funds from the National Institutes of Health shared instrumentation grant program (Grant 1-S10RR13878-01) and the NSF-EPSCOR program for the State of Montana.

■ ABBREVIATIONS

CD, circular dichroism; CPMG, Carr−Purcell−Meiboom−Gill multipulse sequence; CSA, chemical shift anisotropy; DIPSI, decoupling in the presence of scalar interactions; HSQC, heteronuclear single-quantum coherence spectroscopy; IPTG, isopropyl β-thiogalactoside; NMR, nuclear magnetic resonance; Na-EDTA, sodium ethylenediaminetetraacetic acid; NaN_3, sodium azide; nOe, nuclear Overhauser effect; PDB, Protein Data Bank; TrpR, tryptophan repressor; holo-WT-TrpR, wild-type holo-repressor; holo-L75F-TrpR, holo-repressor of the L75F TrpR variant; holo-A77V-TrpR, holo-repressor of the A77V TrpR variant; PMSF, phenylmethanesulfonyl fluoride; WALTZ, Wideband Alternative-phase Low-power Technique for Zero residual splitting.

■ REFERENCES

(1) Klig, L. S., Carey, J., and Yanofsky, C. (1988) Trp repressor interactions with the trp aroH and trpR operators: Comparison of repressor binding in vitro and repression in vivo. *J. Mol. Biol. 202*, 769–777.

(2) Gunsalus, R. P., and Yanofsky, C. (1980) Nucleotide sequence and expression of *Escherichia coli* trpR, the structural gene for the trp apo-repressor. *Proc. Natl. Acad. Sci. U.S.A. 77*, 7117–7121.

(3) Zurawski, G., Gunsalus, R. P., Brown, K. D., and Yanofsky, C. (1981) Structure and regulation of *aroH*, the structural gene for the tryptophan-repressible 3-deoxy-D-arabino-heptulosonic acid-7-phosphate synthetase of *Escherichia coli*. *J. Mol. Biol. 145*, 47–57.

(4) Sarsero, J. P., Wookey, P. J., and Pittard, A. J. (1991) Regulation and expression of *Escherichia coli* K-12 mtr gene by TyrR and trp repressor. *J. Bacteriol. 173*, 4133–4143.

(5) Otwinowski, Z., Schevitz, R. W., Zhang, R. G., Lawson, C. L., Joachimiak, A., Marmorstein, R. Q., Luisi, B. F., and Sigler, P. B. (1988) Crystal structure of trp repressor/operator complex at atomic resolution. *Nature 335*, 321–329.

(6) Schevitz, R. W., Otwinowski, Z., Joachimiak, A., Lawson, C. L., and Sigler, P. B. (1985) The three-dimensional structure of trp repressor. *Nature 317*, 782–786.

(7) Zhang, R. G., Joachimiak, A., Lawson, C. L., Schevitz, R. W., Otwinowski, Z., and Sigler, P. B. (1987) The crystal structure of trp apo-repressor at 1.8 Å shows how binding tryptophan enhances DNA affinity. *Nature 327*, 591–597.

(8) Arrowsmith, C., Pachter, R., Altman, R., and Jardetzky, O. (1991) The solution structures of *Escherichia coli* trp repressor and trp apo-repressor at an intermediate resolution. *Eur. J. Biochem. 202*, 53–66.

(9) Zhao, D., Arrowsmith, C. H., Jia, X., and Jardetzky, O. (1993) Refined solution structures of the *Escherichia coli* trp holo- and apo-repressor. *J. Mol. Biol. 229*, 735–746.

(10) Joachimiak, A., Kelley, R. L., Gunsalus, R. P., Yanofsky, C., and Sigler, P. B. (1983) Purification and characterization of trp apo-repressor. *Proc. Natl. Acad. Sci. U.S.A. 80*, 668–672.

(11) Czaplicki, J., Arrowsmith, C., and Jardetzky, O. (1991) Segmental differences in the stability of the trp repressor peptide backbone. *J. Biomol. NMR 1*, 349–361.

(12) Gryk, M. R., Jardetzky, O., Klig, L. S., and Yanofsky, C. (1996) Flexibility of DNA binding domain of trp repressor required for recognition of different operator sequences. *Protein Sci. 5*, 1195–1197.

(13) Finucane, M. D., and Jardetzky, O. (1995) Mechanism of hydrogen-deuterium exchange in trp repressor studied by ^{1}H-^{15}N NMR. *J. Mol. Biol. 253*, 576–589.

(14) Gryk, M. R., Finucane, M. D., Zheng, Z., and Jardetzky, O. (1995) Solution dynamics of the trp repressor: A study of amide proton exchange by T1 relaxation. *J. Mol. Biol. 246*, 618–627.

(15) Zheng, Z., Czaplicki, J., and Jardetzky, O. (1995) Backbone dynamics of trp repressor studied by ^{15}N NMR relaxation. *Biochemistry 34*, 5212–5223.

(16) Zhang, H., Zhao, D., Revington, M., Lee, W., Jia, X., Arrowsmith, C., and Jardetzky, O. (1994) The solution structures of the trp repressor-operator DNA complex. *J. Mol. Biol. 238*, 592–614.

(17) Hurlburt, B. K., and Yanofsky, C. (1990) Enhanced operator binding by trp superrepressors of *Escherichia coli*. *J. Biol. Chem. 265*, 7853–7858.

(18) Reedstrom, R. J., and Royer, C. A. (1995) Evidence for coupling of folding and function in trp repressor: Physical characterization of the superrepressor mutant AV77. *J. Mol. Biol. 253*, 266–276.

(19) Jin, L., Fukayama, J. W., Pelczer, I., and Carey, J. (1999) Long-range effects on dynamics in a temperature-sensitive mutant of trp repressor. *J. Mol. Biol. 285*, 361–378.

(20) Tyler, R., Pelczer, I., Carey, J., and Copie, V. (2002) Three-dimensional solution NMR structure of Apo-L75F-TrpR, a temperature-sensitive mutant of the tryptophan repressor protein. *Biochemistry 41*, 11954–11962.

(21) Gryk, M. R., and Jardetzky, O. (1996) AV77 hinge mutation stabilizes the helix-turn-helix domain of trp repressor. *J. Mol. Biol. 255*, 204–214.

(22) Schmitt, T. H., Zheng, Z., and Jardetzky, O. (1995) Dynamics of tryptophan binding to *Escherichia coli* Trp repressor wild type and AV77 mutant: An NMR study. *Biochemistry 34*, 13183–13189.

(23) Kelley, R. L., and Yanofsky, C. (1985) Mutational studies with the trp repressor of *Escherichia coli* support the helix-turn-helix model of repressor recognition of operator DNA. *Proc. Natl. Acad. Sci. U.S.A. 82*, 483–487.

(24) Goel, A., Tripet, B. P., Tyler, R. C., Nebert, L. D., and Copie, V. (2010) Backbone amide dynamics of apo-L75F-TrpR, a temperature sensitive mutant of the tryptophan repressor protein (TrpR): Comparison with the ^{15}N NMR relaxation profiles of wild type and A77V mutant TrpR apo-repressors. *Biochemistry 49*, 8006–8019.

(25) Paluh, J. L., and Yanofsky, C. (1986) High level production and rapid purification of the *E. coli* trp repressor. *Nucleic Acids Res. 14*, 7851–7860.

(26) Bodenhausen, G., and Ruben, D. J. (1980) Natural Abundance Nitrogen-15 NMR by Enhanced Heteronuclear Spectroscopy. *Chem. Phys. Lett. 69*, 185–189.

(27) Wittekind, M., and Mueller, L. (1993) HNCACB, a High-Sensitivity 3D NMR Experiment to Correlate Amide-Proton and Nitrogen Resonances with the α- and β-Carbon Resonances in Proteins. *J. Magn. Reson., Ser. B 101*, 201–205.

(28) Grzesiek, S., and Bax, A. (1992) Correlating Backbone Amide and Side-Chain Resonances in Larger Proteins by Multiple Relayed Triple Resonance NMR. *J. Am. Chem. Soc. 114*, 6291–6293.

(29) Delaglio, F., Grzesiek, S., Vuister, G. W., Zhu, G., Pfeifer, J., and Bax, A. (1995) NMRPipe: A Multidimensional Spectral Processing System Based on Unix Pipes. *J. Biomol. NMR 6*, 277–293.

(30) Goddard, T. D., and Kneller, D. G. (2002) *SPARKY 3*, University of California, San Francisco.

(31) Pellecchia, M., Sebbel, P., Hermanns, U., Wuthrich, K., and Glockshuber, R. (1999) Pilus chaperone FimC-adhesin FimH interactions mapped by TROSY-NMR. *Nat. Struct. Biol. 6*, 336–339.

(32) Barbato, G., Ikura, M., Kay, L. E., Pastor, R. W., and Bax, A. (1992) Backbone dynamics of calmodulin studied by ^{15}N relaxation using inverse detected two-dimensional NMR spectroscopy: The central helix is flexible. *Biochemistry 31*, 5269–5278.

(33) Kay, L. E., Torchia, D. A., and Bax, A. (1989) Backbone dynamics of proteins as studied by ^{15}N inverse detected heteronuclear NMR spectroscopy: Application to staphylococcal nuclease. *Biochemistry 28*, 8972–8979.

(34) Grzesiek, S., and Bax, A. (1993) The importance of not saturating H_2O in protein NMR. *J. Am. Chem. Soc. 115*, 12593–12594.

(35) Shaka, A. J., Keeler, J., and Freeman, R. (1983) Evaluation of A New Broad-Band Decoupling Sequence: Waltz-16. *J. Magn. Reson. 53*, 313–340.

(36) Nicholson, L. K., Kay, L. E., Baldisseri, D. M., Arango, J., Young, P. E., Bax, A., and Torchia, D. A. (1992) Dynamics of methyl groups in proteins as studied by proton-detected ^{13}C NMR spectroscopy. Application to the leucine residues of staphylococcal nuclease. *Biochemistry 31*, 5253–5263.

(37) Bracken, C., Carr, P. A., Cavanagh, J., and Palmer, A. G. (1999) Temperature dependence of intramolecular dynamics of the basic leucine zipper of GCN4: Implications for the entropy of association with DNA. *J. Mol. Biol. 285*, 2133–2146.

(38) Bhattacharya, N., Yi, M., Zhou, H.-X., and Logan, T. M. (2007) Backbone dynamics in an intramolecular prolylpeptide-SH3 complex from the diphtheria toxin repressor, DtxR. *J. Mol. Biol. 374*, 977–992.

(39) Lipari, G., and Szabo, A. (1982) ModelFree approach to the interpretation of nuclear magnetic-resonance relaxation in macromolecules. 1. Theory and range of validity. *J. Am. Chem. Soc. 104*, 4546–4559.

(40) Lipari, G., and Szabo, A. (1982) ModelFree approach to the interpretation of nuclear magnetic-resonance relaxation in macromolecules. 2. Analysis of experimental results. *J. Am. Chem. Soc. 104*, 4559–4570.

(41) Cole, R., and Loria, J. P. (2003) FAST-model free: A program for rapid automated analysis of solution NMR spin-relaxation data. *J. Biomol. NMR 26*, 203–213.

(42) Palmer, A. (1998) *ModelFree*, version 4.0, http://cpmcnet.columbia.edu/dept/gsas/biochem/labs/palmer.

(43) Mandel, A. M., Akke, M., and Palmer, A. G. (1995) Backbone dynamics of *Escherichia coli* ribonuclease HI: Correlations with structure and function in an active enzyme. *J. Mol. Biol. 246*, 144–163.

(44) Pawley, N. H., Wang, C., Koide, S., and Nicholson, L. K. (2001) An improved method for distinguishing between anisotropic tumbling and chemical exchange in analysis of ^{15}N relaxation parameters. *J. Biomol. NMR 20*, 149–165.

(45) Tjandra, N., Feller, S. E., Pastor, R. W., and Bax, A. (1995) Rotational diffusion anisotropy of human ubiquitin from N-15 NMR relaxation. *J. Am. Chem. Soc. 117*, 12562–12566.

(46) Hiyama, Y., Niu, C. H., Silverton, J. V., Bavoso, A., and Torchia, D. A. (1988) Determination of ^{15}N chemical shift tensor via ^{15}N-^{2}H dipolar coupling in Boc-glycylglycyl[^{15}N glycine]benzyl ester. *J. Am. Chem. Soc. 110*, 2378–2383.

(47) Farrow, N. A., Zhang, O. W., Szabo, A., Torchia, D. A., and Kay, L. E. (1995) Spectral density function mapping using N-15 relaxation data exclusively. *J. Biomol. NMR 6*, 153–162.

(48) Peng, J. W., and Wagner, G. (1992) Mapping of spectral density functions using heteronuclear NMR relaxation measurements. *J. Magn. Reson. 98*, 308–332.

(49) Kay, L. E. (2005) NMR studies of protein structures and dynamics. *J. Magn. Reson. 173*, 193–207.

(50) Palmer, A. G. (2004) NMR characterization of the dynamics of biomolecules. *Chem. Rev. 104*, 3623–3640.

(51) Boehr, D. D., Dyson, J., and Wright, P. E. (2006) An NMR perspective on enzyme dynamics. *Chem. Rev. 106*, 3055–3079.

(52) Gardino, A. K., and Kern, D. (2007) Functional dynamics of response regulators using NMR relaxation techniques. *Methods Enzymol. 423*, 149–165.

(53) Franzoni, L., Lucke, C., Perz, C., Cavazzini, D., Rademacher, M., Ludwig, C., Spisni, A., and Ruterjans, H. (2002) Structure and backbone dynamics of apo- and holo-cellular retinol-binding protein in solution. *J. Biol. Chem. 277*, 21983–21997.

(54) Zhu, L., Hu, J., Whitson, R., Itakura, K., and Chen, Y. (2001) Dynamics of the Mrf-2 DNA-binding domain free and in complex with DNA. *Biochemistry 40*, 9142–9150.

(55) Dangi, B., Pelupessey, P., Martin, R. G., Rosner, J. L., Louis, J. M., and Gronenborn, A. M. (2001) Structure and dynamics of MarA-DNA complexes: An NMR investigation. *J. Mol. Biol. 314*, 113–127.

(56) Brown, C., Campos-Leon, K., Strickland, M., Williams, C., Fairweather, V., Brady, L. R., Crump, M. P., and Gaston, K. (2011) Protein flexibility directs DNA recognition by the papillomavirus E2 proteins. *Nucleic Acids Res. 39*, 2969–2980.

(57) Swint-Kruse, L., Zhan, H., Fairbanks, B. M., Maheshwari, A., and Matthews., K. S. (2003) Perturbation from a distance: Mutations that alter LacI function through long-range effects. *Biochemistry 42*, 14004–14016.

(58) Xu, J., and Matthews, K. S. (2009) Flexibility in the inducer binding region is crucial for allostery in the *Escherichia coli* lactose repressor. *Biochemistry 48*, 4988–4998.

(59) Flynn, T. C., Swint-Kruse, L., Kong, Y., Booth, C., Matthews, K. S., and Ma, J. (2003) Allosteric transition pathways in the lactose repressor protein core domains: Asymmetric motions in a homodimer. *Protein Sci. 12*, 2523–2541.

(60) Tretyachenko-Ladokhina, V., Ross, J. B. A., and Senear, D. F. (2002) Thermodynamics of *E. coli* cytidine repressor interactions with DNA: Distinct modes of binding to different operators suggest a role in differential gene regulation. *J. Mol. Biol. 316*, 531–546.

(61) Tretyachenko-Ladokhina, V., Cocco, M. J., and Senear, D. F. (2006) Flexibility and adaptability in binding of *E. coli* cytidine repressor to different operators suggests a role in differential gene regulation. *J. Mol. Biol. 362*, 271–286.

(62) Swint-Kruse, L., and Matthews, K. S. (2009) Allostery in the LacI/GalR family: Variations on a theme. *Curr. Opin. Microbiol. 12*, 129–137.

(63) Stacklies, W., Xia, F., and Grater, F. (2009) Dynamic allostery in the methionine repressor revealed by force distribution analysis. *PLoS Comput. Biol. 5*, 1–11.